Published in "Nature 472: 334–337, 2011"
which should be cited to refer to this work.

Stress Transfer in Cellulose Nanowhisker Composites—Influence of Whisker Aspect Ratio and Surface Charge

Rafeadah Rusli,[⊥,‡] Kadhiravan Shanmuganathan,[†] Stuart J. Rowan,[†] Christoph Weder,[†,§] and Stephen J. Eichhorn*[,‡]

[‡]Materials Science Centre and the Northwest Composites Centre, School of Materials, Paper Science Building, Sackville Street, University of Manchester, Manchester, M13 9PL, United Kingdom

[†]Department of Macromolecular Science and Engineering, 2100 Adelbert Road, Kent Hale Smith Building, Case Western University, Cleveland, Ohio 44106, United States

[§]Adolphe Merkle Institute and Fribourg Center for Nanomaterials, University of Fribourg, CH-1700 Fribourg, Switzerland.

ABSTRACT: The mechanically induced molecular deformation of cellulose nanowhiskers embedded in subpercolation concentration in an epoxy resin matrix was monitored through Raman spectroscopy. Cellulose nanowhiskers isolated by sulfuric acid hydrolysis from tunicates and by sulfuric acid hydrolysis and hydrochloric acid hydrolysis from cotton were used to study how the aspect ratio (ca. 76 for tunicate and 19 for cotton) and surface charges (38 and 85 mmol SO_4^-/kg for sulfuric acid hydrolysis of cotton and tunicate, respectively; no detectable surface charges for hydrochloric acid hydrolysis) originating from the isolation process influence stress transfer in such systems. Atomic force microscopy confirmed that uncharged cellulose nanowhiskers produced by hydrochloric acid hydrolysis have a much higher tendency to aggregate than the charged cotton or tunicate nanowhiskers. Each of these nanowhisker types was incorporated in a concentration of 0.7 vol % in a thermosetting epoxy resin matrix. Mechanically induced shifts of the Raman peak initially located at 1095 cm^{-1} were used to express the level of deformation imparted to the nanowhiskers embedded in the resin. Much larger shifts of the diagnostic Raman band were observed for nanocomposites with tunicate nanowhiskers than for the corresponding samples comprising cotton nanowhiskers. In the case of nanocomposites comprising nanowhiskers produced by hydrochloric acid hydrolysis, no significant Raman band shift was observed. These results are indicative of different modes of stress transfer, which in turn appear to originate from the different sample morphologies.

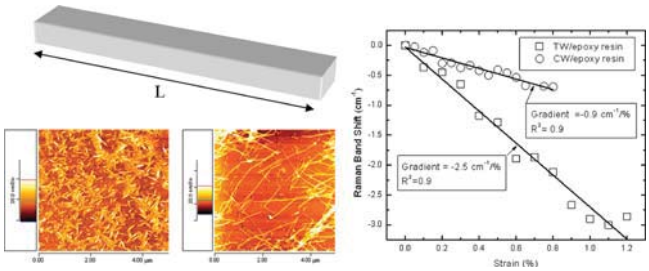

INTRODUCTION

Cellulose nanowhiskers can be produced by acid hydrolysis of cellulose from a variety of plant, animal, and bacterial sources.[1] The process by which this is done selectively hydrolyzes the amorphous material within the cellulose structure, leaving rod-like nanoparticles.[1] The first report on the production of nanostructures of cellulose (then simply termed "crystallites") was published by Ranby in 1951.[2] A similar study was published in 1953 showing how X-ray diffraction could be used to determine the dimensions of these nanoparticles.[3] It was later shown by Marchessault et al. that these nanowhiskers could form birefringent gels and liquid crystalline structures.[4] The liquid crystalline nature of suspensions of these nanowhiskers was further investigated by Revol et al., showing that they formed chiral nematic structures.[5] Since then, a variety of cellulose nanowhisker types have been isolated and studied; these studies are summarized in recent review articles.[1,6,7] A comparison of the dimensions of cellulose nanowhiskers isolated from different sources has also recently been reported.[8] In addition to the plethora of plant-derived cellulose nanowhiskers studied, nanowhiskers isolated from tunicates (a specific family of sea creatures) have attracted considerable attention, due to their exceedingly high aspect ratio. The first report on using cellulose nanowhiskers in a composite material was by Favier et al.[9] who demonstrated that tunicate cellulose nanowhiskers could effectively reinforce a latex material by forming a percolated network. This work was followed by numerous studies of other authors, who demonstrated that cellulose nanowhiskers can provide effective reinforcement for a broad range of polymers.[10] It has been shown that the aspect ratio of these nanowhiskers plays a critical role in their reinforcement potential. In particular, cellulose nanowhiskers produced from *Syngonanthus nitens* have recently been shown to have better reinforcing capability than other plant-derived cellulose nanowhiskers; it has been proposed that this is due to their superior aspect ratio (~67).[11] Tunicate cellulose nanowhiskers are also found to have high aspect ratios,[8] similar to that of *Syngonanthus nitens*, which is also thought to be the reason they exhibit such good reinforcement in composite

materials.[1] Another aspect that could have a significant influence on the reinforcing capability of cellulose nanowhiskers is their surface charge. It is well-known that acid hydrolysis using sulfuric acid generates sulfate ester groups on the surface of the nanowhiskers, imparting negative (anionic) charges.[1,6,7,12] The repulsion among these surface charges appears to moderate the attractive forces due to hydrogen-bonding of the surface alcohol groups, making the nanowhiskers readily dispersible in polar solvents[13] and a broad range of polymers.[10] It is also possible to hydrolyze cellulose to yield uncharged nanowhiskers using hydrochloric acid.[14] Suspensions of neutrally charged nanowhiskers were found to have thixotropic properties at certain concentrations, possibly due to more attractive interactions.[14] These neutrally charged nanowhiskers are typically difficult to disperse well in polymer matrices,[15] although formic acid and *m*-cresol, which have a well-known tendency to break hydrogen bonds, have recently been shown to disperse uncharged tunicate nanowhiskers well.[13]

We report here on the mechanically induced molecular deformation of cellulose nanowhiskers embedded at subpercolation concentration in an epoxy resin matrix, which was monitored through Raman spectroscopy. Cellulose nanowhiskers isolated by sulfuric acid hydrolysis from tunicates and by sulfuric acid hydrolysis and hydrochloric acid hydrolysis from cotton were used, to study how the aspect ratio and surface charges originating from the isolation process influence stress transfer in such systems. Raman spectroscopy has been previously shown to be a powerful tool for probing the local deformation of cellulose nanocomposites.[16−18] The technique relies on following the position of a Raman band, whose original position is characteristic of a main chain vibrational mode. A number of Raman bands have been reported to shift under the action of tensile deformation on cellulosic fibrous materials.[19−24] Here, we exploit this technique to elucidate the stress transfer in nanocomposites comprising different cellulose nanowhiskers with both different aspect ratios and surface charges. Our results are indicative of different modes of stress transfer, which in turn appear to originate from the different sample morphologies. The data suggest that Raman spectroscopic data are a useful diagnostic tool to elucidate the quality of mixing in such nanocomposites.

MATERIAL AND METHODS

Sample Preparation. *Preparation of Cellulose Nanowhiskers.* Tunicates (*Styela clava*) were collected from floating docks at Point View Marina (Narragansett, RI). After gutting, the incrustations on the outer walls of the tunicates were removed by heating at a temperature of 80 °C for 24 h in aqueous potassium hydroxide at 3 L, 5% w/w per 500 g of tunicate walls. This was followed by mechanical agitation, scrubbing, and two more treatments with aqueous potassium hydroxide at 3 L, 5% w/w, and a temperature of 80 °C for 24 h; this protocol represents a minor modification of the procedure reported by Yuan et al.[25] After washing the raw cellulose with water to obtain a neutral solution, 3 L of water, 5 mL of acetic acid, and 10 mL of sodium hypochloric (>4% chlorine) solution were added, and the temperature was raised to 60 °C. In one-hour intervals, additional portions at 5 mL of acetic acid and 10 mL of sodium hypochlorite solution (>4% chlorine) were added until the material's color changed from pinkish to pure white (usually two or three additions were required, depending on the particular batch of tunicates). Finally, the bleached deproteinized walls were washed with deionized water and disintegrated with a Waring blender, yielding a fine cellulose pulp. Sulfate functionalized tunicate nanowhiskers were prepared by H_2SO_4 hydrolysis of cellulose pulp, according to the method described by Favier et al.[9] with slight modifications. Thus, 960 mL of 98% sulfuric acid was slowly added under vigorous mechanical stirring to a cooled suspension of tunicate cellulose pulp in 600 mL of deionized water at 0 °C. This dispersion was then heated to 60 °C and maintained at that temperature for 20 min while continually stirring. The dispersion was cooled to 0 °C, filtered over a small-pore fritted glass filter, and washed with deionized water until neutrality was reached. Finally, the sulfonated tunicate nanowhiskers were dispersed in 1 L of deionized water by overnight sonication and were then freeze−dried.

Cotton cellulose nanowhiskers were prepared from sulfuric acid (H_2SO_4) hydrolysis of Whatman filter paper. About 40 g of the filter paper was added to 700 mL 64% w/w H_2SO_4 (>95%, Fisher Scientific) at 45 °C for 45 min. The suspension was diluted 5-fold with deionized water, then concentrated and rinsed by centrifugation (Centrifuge Sigma U-16, Sci-Quip) at 6000 rpm for 10 min, followed by dialysis against water until they were neutralized. Then, the suspension was treated with mixed bed ion-exchange resin (Amberlite MB 6113, Fluka) and filtered using Whatman glass microfiber filters. The suspension was sonicated (Branson Digital Sonifier) repeatedly to produce cellulose nanowhiskers of colloidal dimensions. The concentration of the suspension was 1.8 ± 0.2% by weight. Freeze−drying of the nanowhiskers then took place prior to preparation of the composites.

In order to prepare hydrochloric acid hydrolyzed nanowhiskers, Whatman filter paper (10 g) was hydrolyzed in 300 mL of 4 N hydrochloric acid (HCl) (reagent grade 37%, Sigma Aldrich). The mixture was stirred continuously at 80 °C for 225 min. The nanowhisker suspension was then centrifuged at 1600 *g* for 5 min. The process was repeated until the pH of the suspension reached a value of 4−5 and then dialyzed against deionized water to neutrality. The suspension was sonicated for 1 min. Freeze−drying of the nanowhiskers then took place prior to preparation of the composites.

Cellulose Nanocomposite Preparation. Support beams of the neat epoxy resin composites were prepared by mixing the Araldite epoxy resin LY5052 and hardener HY5052 (both Huntsman), using a ratio of 50 g of resin to 19 g of hardener. This epoxy system was chosen due to its low fluorescence and because carbon nanotube-containing nanocomposites based on this cold-cured system were shown to exhibit only minimal residual stresses.[26] The density of this epoxy resin is around 1.1 g cm^{-3}.[27] Resin and hardener were mixed and stirred thoroughly. Since this caused the formation of small bubbles, the mixture was degassed in a thermostat vacuum oven (Townson and Mercer Ltd.) at room temperature and a pressure of 30 mmHg for 30 min. The resin was then poured carefully into a mold and left to cure for 7 days at room temperature. The cured epoxy resin sheet was then cut into beams with dimensions of 80 × 10 × 3 mm^3 using a band saw. Using this pure epoxy beam as a base, two different types of method were used to secure a whisker-resin formulation to the beam, as follows:

- For the cotton cellulose nanowhiskers, a thin layer of epoxy resin and nanowhiskers was cured onto these beams in order to minimize the amount of resin through which the laser had to penetrate in order to obtain a signal from the cellulose.
- For the tunicate cellulose nanowhiskers, a thin sheet of whiskers and resin was precured and cut into strips and secured to the beam using further epoxy resin.

The freeze−dried cotton cellulose nanowhiskers isolated by sulfuric acid hydrolysis were dispersed in the hardener using an ultrasonic bath (Scientific Laboratory Supplies) and an ultrasound sonifier (Digital Sonifier, Branson Ultrasonics) for 6 h. This mixture was then blended with the epoxy resin (at the same ratio as for the support beams) and was then stirred carefully to avoid the formation of bubbles. The volume fraction of the nanowhiskers in the resin was 0.7% v/v. The viscous mixture was then layered onto the surface of the epoxy resin support beams and left to cure for seven days at room temperature. The thickness

Table 1. Mean Diameters, Lengths, and Aspect Ratios for Sulfuric Acid Hydrolyzed Tunicate Cellulose Nanowhiskers, Sulfuric Acid Hydrolyzed Cotton Cellulose Nanowhiskers, and Hydrocholoric Acid Hydrolyzed Cotton Cellulose Nanowhiskers

	diameter (nm)	length (nm)	aspect ratio
H_2SO_4 hydrolyzed tunicate cellulose nanowhiskers	8 ± 2	1525 ± 843	76 ± 46
H_2SO_4 hydrolyzed cotton cellulose nanowhiskers	13 ± 2	138 ± 42	19 ± 6
HCl hydrolyzed cotton cellulose nanowhiskers	19 ± 6	350 ± 101	19 ± 8

of the cured nanocomposite layer on the support beam was ~1 mm. The same approach was adopted for nanowhiskers isolated by hydrochloric acid hydrolysis. In the case of tunicate nanowhiskers, a similar method was used; in this case, the nanocomposite was cured as a sheet. A thin strip (1 × 1 cm, and ~1 mm thick) of the nanocomposite was cut from this sheet once curing had been completed, and the nanocomposite strip was secured to the surface of a support beam by applying a small amount of the neat epoxy resin. A strain gauge (type EA-06-240LZ-120, Vishay Micro-Measurements) of gauge factor 2.08 was attached to the surface of the epoxy resin support beams close to the nanocomposites using a small drop of cyanoacrylate adhesive.

Conductometric Titration. Conductometric titrations were performed on suspensions of the cellulose nanowhiskers produced by H_2SO_4 and HCl hydrolysis to quantify the surface charges. About 3 mL of weighed cellulose nanowhisker suspension was poured into a 100 mL three-necked round-bottomed flask. Then, 100 mL of 0.01 mM sodium chloride solution (NaCl) (Fisher Scientific) was added into the suspension and the mixture was stirred continuously. The suspension was titrated using 0.002 M sodium hydroxide (NaOH) (Fisher Scientific). The resistance of the suspension was monitored using a resistance meter (6401 LCR Databridge, Tinsley Prism Instruments). These data were then inverted to obtain the actual conductivity of the suspension. All titrations were repeated 3 times and the quoted values are averages. The surface charges (expressed as sulfur content, assuming that charges are present as OSO_3^- groups) were calculated from the added volume of NaOH by using the equation according to Dong et al.[28]

$$s\,(\%) = \frac{32NV}{w_t W} \qquad (1)$$

where N and V are the concentration and volume of added NaOH, w_t is the weight of added suspension, and W is the weight percentage concentration of the nanowhisker suspension.

Atomic Force Microscopy. The samples were prepared by spin-coating 0.1% aqueous cellulose nanowhisker suspensions that were made by redispersing freeze−dried nanowhiskers through ultrasonication (Digital Sonifier, Branson Ultrasonics) for 6 h. Silicon wafers which had been cut into 1.0 × 1.0 cm^2 pieces and cleaned using piranha solution (3:1, sulfuric acid to hydrogen peroxide, Sigma Aldrich) for 30 min were used as substrates. The spin-coating was carried out with a Laurell Technologies Corporation spin-coater (model WS 650SZ) using a speed of 4000 rpm and an acceleration of 2125 rpm s^{-1}. The spinning was retained for 30 s. This method is based on the work of Kontturi et al.[29]

Atomic force microscopy (AFM) measurements were performed with a Digital Instruments CP-II from Veeco Instruments Ltd. at room temperature. The measurements and images were obtained simultaneously in tapping mode at the fundamental resonance frequency of the cantilever with a scan rate of 0.5 lines s^{-1}. The *Image Processing and Data Analysis* v 2.1.15 software was used to process the AFM images and determine diameters and lengths of the nanowhiskers. Due to tip broadening effects, the height of the nanowhiskers was used to determine mean diameters. Tip broadening effects also cause an error in the length measurements, but this was unavoidable.

Molecular Deformation Studies Using Raman Spectroscopy. A Renishaw System 1000 Raman spectrometer coupled to an Olympus microscope was used to collect spectra from the nanocomposite samples during tensile and compressive deformation. Nanocomposite-coated support beams were deformed on a customized 4-point bending rig both in tension and in compression. The laser (λ = 785 nm) was focused to a spot size of 2 μm using the microscope and a 50× objective lens (numerical aperture = 0.60). Spectra were recorded using an exposure time of 120 s and the laser polarization was parallel to the strain axis of the samples. A mixed Gaussian/Lorentzian function, and an algorithm based on the work of Marquardt,[30] were used to fit spectra in order to find their position.

RESULTS AND DISCUSSION

Conductometric Titration and Charge Density. The concentration of the sulfate groups on the cellulose nanowhiskers was determined from the conductometric titrations of aqueous nanowhisker suspensions. A typical titration curve for the sulfuric acid hydrolyzed cotton nanowhisker suspension is shown in Figure 1a (similar curves were obtained for the tunicate samples). The curve shows a decrease in conductivity caused by the neutralization of strong acid groups on the surface of the cellulose nanowhiskers. There is a plateau region after the point of inflection, which relates to the neutralization of weak acid groups (carboxylic acid). Once the neutralization was completed, the increase in conductivity could be seen due to the excess alkali. The cotton nanowhiskers produced by acid hydrolysis using sulfuric acid exhibited lower charge concentration (~38 mmol SO_4^- kg^{-1} cellulose). Tunicate nanowhiskers were found to have concentrations of negatively charged groups of ~85 mmol SO_4^- kg^{-1} cellulose which explains the good dispersibility of tunicate nanowhiskers in DMF[31] and may be partly responsible for the swelling behavior of tunicate nanowhisker/PVAc nanocomposites.[32,33] Assuming cylindrical geometries for the nanowhiskers and using the nanowhisker dimensions given in Table 1, the surface area to volume ratio of tunicate nanowhiskers (0.50) is ~2.5 times higher than that of the cotton derived nanowhiskers (0.20). The surface charge densities are thought to be comparable, within the error of the experiment, for the two whisker types. An estimation of the surface charge densities can be determined by assuming that the tunicate and cotton nanowhiskers consist of 10 × 10 and 16 × 16 arrays of chains, respectively, given their respective diameters. In each case, a proportion (36% and 23%, respectively, for tunicate and cotton) are surface chains. Given that about 1 kg of cellulose is about 6.17 mol of glucose residues, values of 0.038 and 0.026 SO_4^- groups per glucose residue are obtained for tunicate and cotton, respectively.

The titration curve of the hydrochloric acid hydrolyzed cotton nanowhisker suspension shows an increase of conductivity from the very beginning, without any decrease in the conductivity (Figure 1b). This confirms that there are no strong acid groups present on the surface of these cellulose nanowhiskers.

AFM Imaging of Nanowhiskers. Representative AFM images of the nanowhiskers are shown in Figure 2. An image

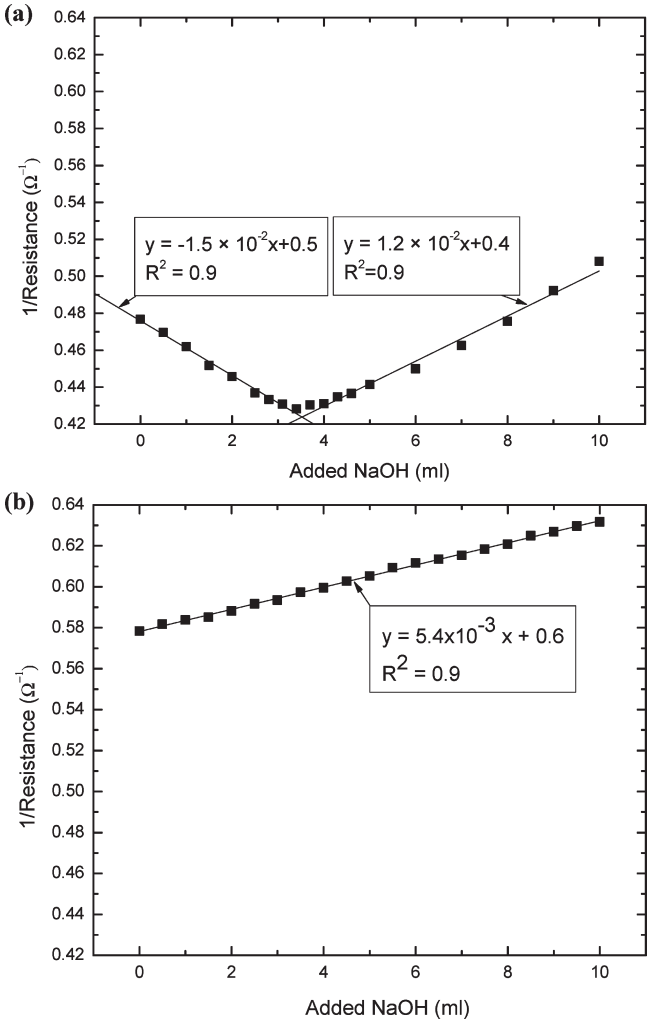

Figure 1. Conductometric titration curves (resistivity versus added sodium hydroxide) for (a) cotton derived cellulose nanowhiskers produced using sulfuric acid hydrolysis and (b) cotton derived cellulose nanowhiskers produced using hydrochloric acid hydrolysis. Solid lines are linear regressions to the data.

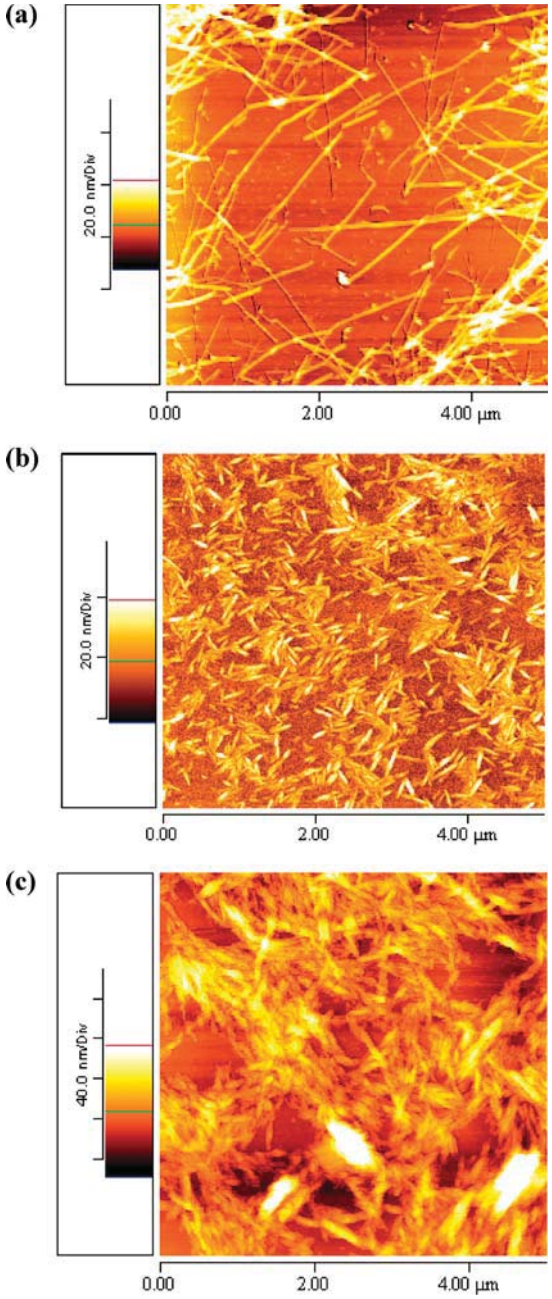

Figure 2. Atomic force microscopy (AFM) images of cellulose nanowhiskers: (a) tunicate nanowhiskers produced by hydrolysis with sulfuric acid, (b) cotton nanowhiskers produced by hydrolysis with sulfuric acid, and (c) cotton nanowhiskers produced by hydrolysis with hydrochloric acid. The samples were spin-coated from aqueous dispersions containing 0.1% v/v of redispersed freeze−dried nanowhiskers.

of the nanowhiskers produced by sulfuric acid hydrolysis of tunicates is shown in Figure 2a. The image reveals that these nanowhiskers are long and slender. Moderate aggregation of the tunicate nanowhiskers is also evident, which is most likely to due to the drying process employed during the preparation of the sample. In Figure 2b, an image of nanowhiskers produced by sulfuric acid hydrolysis of cotton is shown. This image shows that these nanowhiskers are shorter and wider than those isolated from tunicates and suggests a somewhat higher tendency for aggregation. Finally, an image of nanowhiskers produced by acid hydrolysis of cotton using hydrochloric acid is shown in Figure 2c. This image shows that these nanowhiskers are highly aggregated, making it difficult to differentiate individual nanowhiskers. This high level of aggregation is thought to be due to the lack of surface charges leading to strong interactions between nanowhiskers on account of hydrogen bonding between the surface hydroxyl groups. The significant level of aggregation made the determination of the dimensions of hydrochloric acid hydrolyzed nanowhiskers somewhat challenging. Nevertheless, mean values (determined from 30 independent measurements) were obtained for the lengths and diameters of each nanowhisker type. In order to do this, it was assumed that they had an axisymmetric morphology. These values are reported in Table 1, along with the calculated aspect ratios A (length/diameter). The errors reported for the aspect ratio were calculated using the propagation of error formula

$$\Delta(A) = A\sqrt{\left(\frac{\Delta D}{D}\right)^2 + \left(\frac{\Delta L}{L}\right)^2} \qquad (2)$$

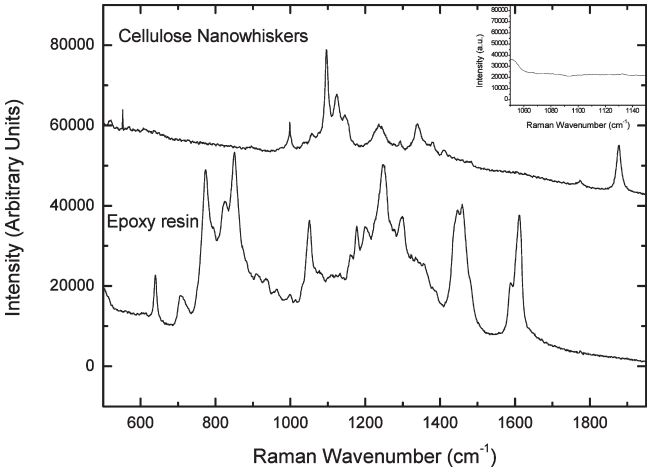

Figure 3. Typical Raman spectra for sulfuric acid hydrolyzed tunicate cellulose nanowhiskers and the epoxy resin employed. Inset shows Raman spectrum of epoxy resin in the region 1050−1150 cm^{-1}.

where A is the aspect ratio, and ΔD and ΔL are the errors on the diameters (D) and lengths (L) of the nanowhiskers, respectively. It is worth noting that these errors are high, which is due to the difficulty of measuring the dimensions of the nanowhiskers due to overlap and aggregation.

Consistent with previous studies of van der Berg et al.[34] cellulose nanowhiskers derived from tunicates have a much greater aspect ratio (∼76) than those derived from cotton (∼19). Hydrochloric acid hydrolyzed cotton cellulose nanowhiskers were found to be about twice as long as sulfuric acid produced cotton nanowhiskers. They also have broader size distributions, perhaps due to the fact that they were aggregated, as a consequence of the lack of surface charges. The increased width may be due to side-by-side aggregation, out of the plane of the image, of individual whiskers not readily resolved from the images. Similar aspect ratio values are however obtained for both types of cotton cellulose nanowhiskers.

Raman Spectroscopy and Molecular Deformation. Typical Raman spectra obtained from a solution-cast film of the neat cellulose nanowhiskers isolated by sulfuric acid hydrolysis from tunicates and from the neat epoxy resin are shown in Figure 3. Similar spectra were obtained for the cotton cellulose nanowhiskers, and have indeed been reported elsewhere.[18,35] It is clear from these spectra that no interference from the spectrum for the epoxy resin with the main vibration located at approximately 1095 cm^{-1} from the cellulose nanowhiskers occurs. This enables the monitoring of the position of this band with deformation. Typical shifts in the position of this peak (in tension) are shown in Figure 4a,b for nanocomposites based on the epoxy matrix and sulfuric acid hydrolyzed tunicate and cotton cellulose nanowhiskers, respectively. It is well-known that the Raman peak located at 1095 cm^{-1} corresponds to C−O stretching, both within the ring[36] and along the glycosidic linkage.[22,37] Therefore, a shift in the position of this peak upon deformation, as shown in Figure 4, represents direct deformation along the backbone of the cellulose polymer. A comparison between the shifts as a function of tensile strain observed for nanocomposites of the epoxy resin and sulfuric acid hydrolyzed tunicate and cotton cellulose nanowhiskers is shown in Figure 5. Linear fits to these data are also shown; the gradients thus established are representative for the level of deformation of the nanowhiskers, and therewith indirectly also

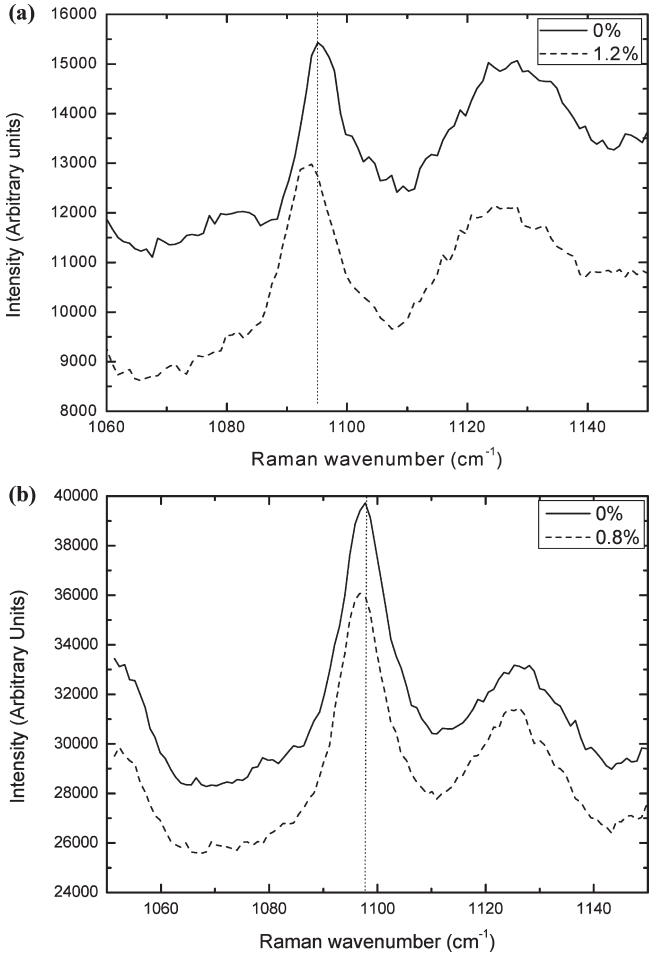

Figure 4. Typical shifts of the position of the Raman band located at 1095 cm^{-1} upon tensile deformation of nanocomposites of the epoxy resin and 0.7% v/v: (a) tunicate cellulose nanowhiskers and (b) cotton cellulose nanowhiskers, both isolated by sulfuric acid hydrolysis. Shown are spectra of undeformed samples (0%, solid lines), and samples that were elongated under uniaxial stress by 1.2% (a) and 0.8% (b), respectively (dashed lines).

the stress transfer within the composite. It is clear that a greater level of deformation occurs in the tunicate−epoxy nanocomposite, compared to the cotton nanowhisker based samples. In a recent comparative study by Tang and Weder,[31] better reinforcement of an epoxy resin using tunicate nanowhiskers compared to cotton has been reported, where the enhancement was particularly noticeable above the glass transition temperature of the resin.[31] For both nanowhisker types, the reinforcement effect was attributed to the formation of a percolating nanowhisker network, in which stress is assumed to be transferred primarily through whisker−whisker interactions.[31] It must be stressed that the nanocomposites studied here had a nanowhisker volume fraction of 0.7% v/v, which is below the percolation concentration. Therefore, the stress transfer in the present systems, in contrast to the previously studied systems, is thought not to involve a nanowhisker network, in which stress is transferred through whisker−whisker interactions,[31] but will rely primarily on whisker−matrix interactions.

Nanocomposite samples of an epoxy resin containing cotton cellulose nanowhiskers produced by hydrolysis using hydrochloric acid were also analyzed using the same Raman spectroscopic

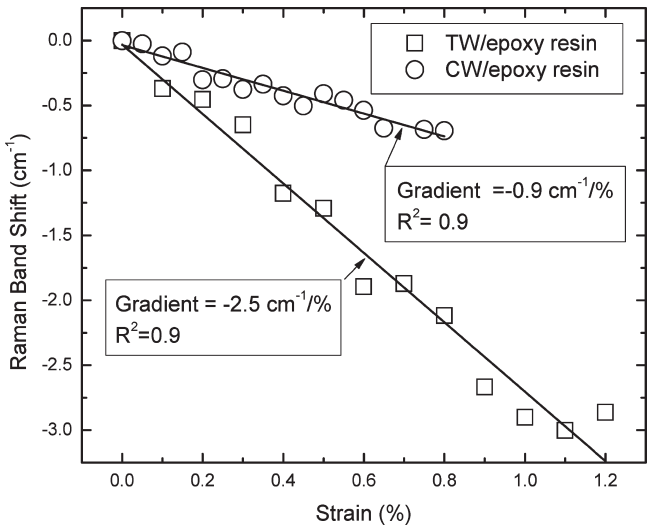

Figure 5. Typical shifts of the position of the Raman band located at 1095 cm^{-1} upon tensile deformation of nanocomposites of the epoxy resin and 0.7% v/v tunicate cellulose nanowhiskers (TW, squares) and 0.7% v/v cotton cellulose nanowhiskers (CW, circles), both isolated by sulfuric acid hydrolysis. Shown are the variations of the Raman band location upon elongation of the samples under uniaxial stress to the strains indicated in the figure. Solid lines are linear regressions to the data.

method. Data from these samples are reported in Figure 6a, with data from the sulfuric acid hydrolyzed nanowhiskers for comparison. No detectable shift in the position of the Raman peak located at 1095 cm^{-1} is observed for the nanocomposites containing hydrochloric acid hydrolyzed nanowhiskers when they are deformed in tension (Figure 6a). This result suggests that aggregation of the nanowhiskers, as seen in the AFM images of the neat whiskers, also occurs in the nanocomposites leading to lower stress transfer efficiency. An aggregation of nanowhiskers will effectively reduce the aspect ratio of the reinforcing phase leading to a lower stress-transfer efficiency. In addition to this, it will also reduce the surface area that is effectively in contact with the resin resulting in a reduction in stress transfer. It is clear therefore that the charge on the surface of the nanowhiskers indirectly plays a key role in the interfacial mechanics of these materials.

Figure 6b shows the shift in the Raman band located initially at 1095 cm^{-1} upon compressing nanocomposites containing sulfuric acid and hydrochloric acid hydrolyzed nanowhiskers. The data mirror the results of the tensile deformation experiments. In the case of the sulfuric acid hydrolyzed cellulose nanowhisker-based nanocomposite, the Raman peak located at 1095 cm^{-1} shifts toward a *higher* wavenumber position upon compression to reach a plateau at about 0.8% compressive strain. A similar result has been previously reported for cellulose nanowhisker composites[16] and has been attributed to a buckling mechanism. Gratifyingly, the gradient of the data, derived from the linear regression, is similar in magnitude to the tensile data (cf. 0.9 cm^{-1} $\%^{-1}$ in Figure 6a with 0.8 cm^{-1} $\%^{-1}$ in Figure 6b) which suggests that the stress transfer mechanisms in compression and tension are the same. As for experiments conducted under tension, only a negligible Raman band shift can be observed for the nanocomposites containing cellulose nanowhiskers derived from hydrochloric acid hydrolysis; a similar result is

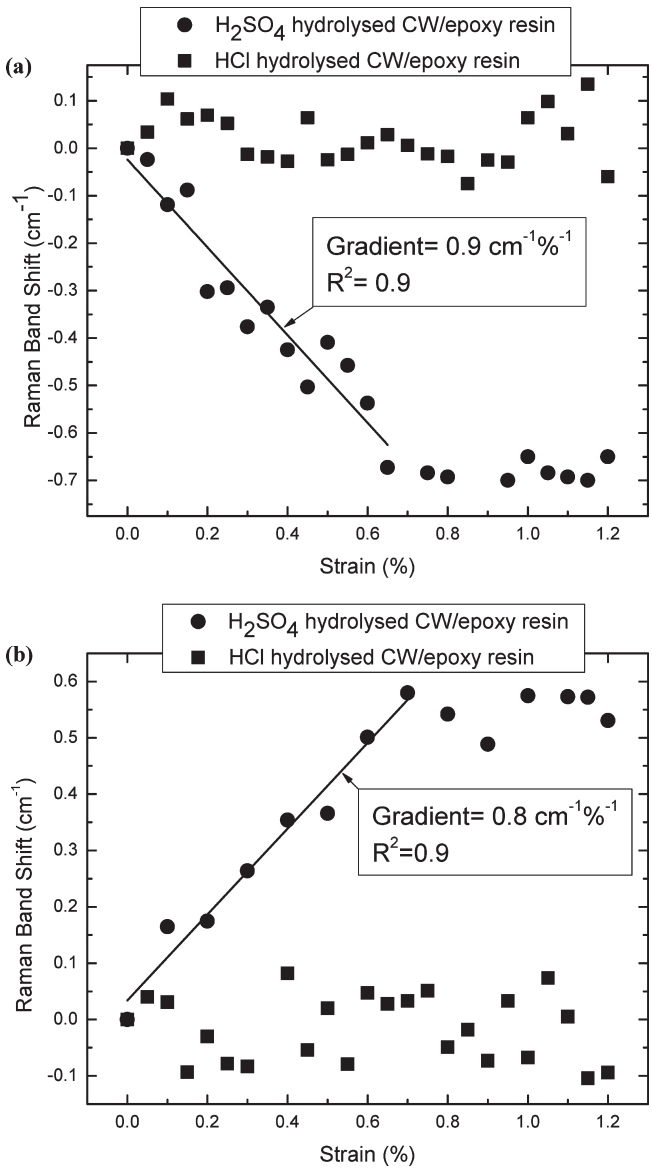

Figure 6. Typical shifts of the position of the Raman band located at 1095 cm^{-1} upon deformation of nanocomposites of the epoxy resin and 0.7% v/v cotton cellulose nanowhiskers isolated by hydrolysis with hydrochloric acid and sulfuric acid, respectively. Shown are the variations of the Raman band location upon (a) elongating the samples under uniaxial stress to the strains indicated in the figure and (b) compressing the samples to various strains. Solid lines are linear regressions to the data.

obtained in compression. This lack of stress transfer is thought to be due to the aggregation of the whiskers and a reduction in the effective aspect ratio.

CONCLUSIONS

The mechanically induced molecular deformation of cellulose nanowhiskers embedded in subpercolation concentration in an epoxy resin matrix was monitored through Raman spectroscopy. Cellulose nanowhiskers isolated by sulfuric acid hydrolysis from tunicates and by sulfuric acid hydrolysis and hydrochloric acid hydrolysis from cotton were used to study how the aspect ratio and surface charges originating from the isolation process

influence stress transfer in such systems. The greatest level of stress transfer was observed in the sulfuric acid hydrolyzed tunicate nanowhisker-based nanocomposites followed by nanocomposites based on sulfuric acid hydrolyzed cotton-derived nanowhiskers. This is thought to be due to the higher aspect ratio of the tunicate nanowhiskers. It has also been shown that the lack of surface charges on the hydrocholoric acid derived nanowhiskers leads to negligible stress transfer, which is attributed to their aggregation and subsequent reduction in effective aspect ratio and surface area. These findings demonstrate the importance of surface charges, which—perhaps counterintuitively, as they reduce the interactions between whiskers—have a beneficial influence on the mechanical properties of these materials. The data suggest that Raman spectroscopic data are a useful diagnostic tool to elucidate the quality of mixing in such nanocomposites.

AUTHOR INFORMATION

Corresponding Author

*E-mail: s.j.eichhorn@manchester.ac.uk. Telephone: 0161 306 5982, Fax: 0161 306 3586.

Present Addresses

⊥Forestry Research Institute Malaysia (FRIM), 52110 Kepong, Selangor Darul Ehsan, Kuala Lumpur, Malaysia.

ACKNOWLEDGMENT

The authors wish to thank the Ministry of Science, Technology and Innovation, Malaysia for funding a PhD studentship (to R.R.), the National Science Foundation under Grants No. DMR-0804874 and CBET-0828155, Case Western Reserve University for an Ohio Innovation Incentive Fellowship (to K.S.), and the Adolphe Merkle Foundation.

REFERENCES

(1) Eichhorn, S. J. *Soft Matter* **2011**, *7*, 303–315.
(2) Ranby, B. G. *Discuss. Faraday Soc.* **1951**, *11*, 158–164.
(3) Mukherjee, S. M.; Woods, H. J. *Biochim. Biophys. Acta* **1953**, *10* (4), 499–511.
(4) Marchessault, R. H.; Morehead, F. F.; Walter, N. M. *Nature* **1959**, *184* (4686), 632–633.
(5) Revol, J. F.; Bradford, H.; Giasson, J.; Marchessault, R. H.; Gray, D. G. *Int. J. Biol. Macromol.* **1992**, *14* (3), 170–172.
(6) Habibi, Y.; Lucia, L. A.; Rojas, O. J. *Chem. Soc. Rev.* **2010**, *110* (6), 3479–3500.
(7) Lima, M. M. D.; Borsali, R. *Macromol. Rapid Commun.* **2004**, *25* (7), 771–787.
(8) Elazzouzi-Hafraoui, S.; Nishiyama, Y.; Putaux, J. L.; Heux, L.; Dubreuil, F.; Rochas, C. *Biomacromolecules* **2008**, *9* (1), 57–65.
(9) Favier, V.; Chanzy, H.; Cavaille, J. Y. *Macromolecules* **1995**, *28* (18), 6365–6367.
(10) Eichhorn, S. J.; Dufresne, A.; Aranguren, M.; Marcovich, N. E.; Capadona, J. R.; Rowan, S. J.; Weder, C.; Thielemans, W.; Roman, M.; Renneckar, S.; Gindl, W.; Veigel, S.; Keckes, J.; Yano, H.; Abe, K.; Nogi, M.; Nakagaito, A. N.; Mangalam, A.; Simonsen, J.; Benight, A. S.; Bismarck, A.; Berglund, L. A.; Peijs, T. *J. Mater. Sci.* **2010**, *45* (1), 1–33.
(11) Siqueira, G.; Abdillahi, H.; Bras, J.; Dufresne, A. *Cellulose* **2010**, *17* (2), 289–298.
(12) Azizi Samir, M. A. S.; Alloin, F.; Dufresne, A. *Biomacromolecules* **2005**, *6* (2), 612–626.
(13) van den Berg, O.; Capadona, J. R.; Weder, C. *Biomacromolecules* **2007**, *8* (4), 1353–1357.
(14) Araki, J.; Wada, M.; Kuga, S.; Okano, T. *Colloids Surf., A* **1998**, *142* (1), 75–82.
(15) Saxena, A.; Elder, T. J.; Pan, S.; Ragauskas, A. J. *Composites, Part B* **2009**, *40* (8), 727–730.
(16) Rusli, R.; Eichhorn, S. J. *Appl. Phys. Lett.* **2008**, *93* (3), 3.
(17) Rusli, R.; Shanmuganathan, K.; Rowan, S. J.; Weder, C.; Eichhorn, S. J. *Biomacromolecules* **2010**, *11* (3), 762–768.
(18) Sturcova, A.; Davies, G. R.; Eichhorn, S. J. *Biomacromolecules* **2005**, *6* (2), 1055–1061.
(19) Hamad, W. Y.; Eichhorn, S. *ASME J. Eng. Mater. Technol.* **1997**, *119* (3), 309–313.
(20) Eichhorn, S. J.; Hughes, M.; Snell, R.; Mott, L. *J. Mater. Sci. Lett.* **2000**, *19* (8), 721–723.
(21) Young, R. J.; Eichhorn, S. J. *Polymer* **2007**, *48* (1), 2–18.
(22) Gierlinger, N.; Schwanninger, M.; Reinecke, A.; Burgert, I. *Biomacromolecules* **2006**, *7* (7), 2077–2081.
(23) Peetla, P.; Schenzel, K. C.; Diepenbrock, W. *Appl. Spectrosc.* **2006**, *60* (6), 682–691.
(24) Tze, W. T. Y.; O'Neill, S. C.; Tripp, C. P.; Gardner, D. J.; Shaler, S. M. *Wood Fiber Sci.* **2007**, *39* (1), 184–195.
(25) Yuan, H.; Nishiyama, Y.; Wada, M.; Kuga, S. *Biomacromolecules* **2006**, *7* (3), 696–700.
(26) Kao, C. C.; Young, R. J. *J. Mater. Sci.* **2010**, *45* (6), 1425–1431.
(27) Davies, R. J.; Riekel, C.; Bennett, J. A.; Eichhorn, S. J.; Young, R. J. *Appl. Phys. Lett.* **2007**, *91*, (4), -.
(28) Dong, X. M.; Revol, J. F.; Gray, D. G. *Cellulose* **1998**, *5*, 19–32.
(29) Kontturi, E.; Johansson, L.; Katri S. Kontturi, K. S.; Ahonen, P.; Thüne, P. C.; Laine, J. *Langmuir* **2007**, *23*, 9674–9680.
(30) Marquardt, D. W. *J. Soc. Ind. Appl. Math.* **1963**, *11* (2), 431–441.
(31) Tang, L. M.; Weder, C. *ACS Appl. Mater. Interfaces* **2010**, *2* (4), 1073–1080.
(32) Capadona, J. R.; Shanmuganathan, K.; Tyler, D. J.; Rowan, S. J.; Weder, C. *Science* **2008**, *319* (5868), 1370–1374.
(33) Shanmuganathan, K.; Capadona, J. R.; Rowan, S. J.; Weder, C. *J. Mater. Chem.* **2010**, *20* (1), 180–186.
(34) van der Berg, O.; Capadona, J. R.; Weder, C. . *Biomacromolecules* **2007**, *8* (4), 1353–1357.
(35) Rusli, R.; Eichhorn, S. J. *Appl. Phys. Lett.* **2008**, *93* (3), 033111.
(36) Wiley, J. H.; Atalla, R. H. *Carbohydr. Res.* **1987**, *160*, 113–129.
(37) Edwards, H. G. M.; Farwell, D. W.; Webster, D. *Spectrochim. Acta, Part A* **1997**, *53* (13), 2383–2392.